Resolution of Fluorescence Correlation Measurements

Ulrich Meseth,* Thorsten Wohland,* Rudolf Rigler,# and Horst Vogel*
*Department of Chemistry, LCPPM, Swiss Federal Institute of Technology, CH-1015 Lausanne, Switzerland; and #Institute of Medical Biophysics, Karolinska Institute, Doktorsringen 6C 3H, 10401 Stockholm, Sweden

ABSTRACT The resolution limit of fluorescence correlation spectroscopy for two-component solutions is investigated theoretically and experimentally. The autocorrelation function for two different particles in solution were computed, statistical noise was added, and the resulting curve was fitted with a least squares fit. These simulations show that the ability to distinguish between two different molecular species in solution depends strongly on the number of photons detected from each particle, their difference in size, and the concentration of each component in solution. To distinguish two components, their diffusion times must differ by at least a factor of 1.6 for comparable quantum yields and a high fluorescence signal. Experiments were conducted with Rhodamine 6G and Rhodamine-labeled bovine serum albumin. The experimental results support the simulations. In addition, they show that even with a high fluorescence signal but significantly different quantum yields, the diffusion times must differ by a factor much bigger than 1.6 to distinguish the two components. Depending on the quantum yields and the difference in size, there exists a concentration threshold for the less abundant component below which it is not possible to determine with statistical means alone that two particles are in solution.

INTRODUCTION

Fluorescence correlation spectroscopy (FCS) uses statistical fluctuations in the fluorescence intensity of a small illuminated sample volume to obtain information about the processes that provoke these fluctuations. It is an easily applied optical method that was introduced more than two decades ago (Ehrenberg and Rigler, 1974; Ehrenberg and Rigler, 1976; Elson and Madge, 1974; Madge et al., 1974) and has been reviewed by several authors (Rigler et al., 1992; Thompson, 1991; Widengren, 1996). Originally designed to measure diffusion coefficients and concentrations of fluorescently labeled molecules, it has since been used to measure a wide range of parameters. The measured quantities include translational diffusion (Elson et al., 1974; Madge et al., 1974), rotational motion (Aragon and Pecora, 1976; Ehrenberg et al., 1974; Ehrenberg et al., 1976; Kask et al., 1989), chemical kinetics (Icenogle and Elson, 1983; Madge et al., 1974), fluorescence lifetime of the excited state (Basché, 1996; Kask et al., 1985; Widengren et al., 1994), diffusion and interactions between molecules (Klingler and Friedrich, 1997; Rauer et al., 1996), and aggregation and self-association (Hinterdorfer et al., 1997; Meyer and Schindler, 1988). To reduce background noise, two-photon excitation has been applied to FCS (Berland et al., 1995). Fluorescence correlation was measured not in time but over space in combination with a scanning confocal microscope to determine the distribution of proteins in supported planar membranes (Huang and Thompson, 1996).

The statistical accuracy of FCS measurements has been treated theoretically by several authors (Kask et al., 1997; Koppel, 1974; Qian, 1990). However, these discussions did not address the question of the practical resolution limit attainable by FCS experiments in systems containing more than one component. This resolution limit is of great importance for measurements of biological systems where binding and aggregation play an essential role for proper functioning. The binding of ligands to receptors can only be quantified when the fluorescently labeled bound ligand can be clearly distinguished from the free ligand (Rauer et al., 1996), i.e., if the diffusion coefficients are sufficiently different. The same argument applies for aggregation, which can only be measured if aggregates can be distinguished from monomers. The ability to distinguish two particles in solution is determined by the attainable resolution of correlation times in the FCS experiments. In this paper we will examine theoretically and experimentally to what degree of accuracy translational diffusion can be measured in single- and two-component systems. This limit in turn will determine the extent to which binding and aggregation can be measured. For simulated time correlation curves we calculated autocorrelation functions (ACF), added statistical noise, and fitted the resulting synthetic curve with a least squares fit. In addition, real FCS experiments were performed with mixtures of Rhodamine 6G (Rho 6G) and bovine serum albumin labeled by tetramethyl-rhodamine isothiocyanate (Rho-BSA). The experimental correlation curves were evaluated by the same fit procedures used for the synthetic curves. This approach shows that the predictions of the theory are in accordance with the experimental results and in addition gives empirical limits whether two particles in solution can be distinguished only on the basis

Received for publication 10 August 1998 and in final form 18 December 1998.

Address reprint requests to Dr. Horst Vogel, Department of Chemistry, LCPPM, Swiss Federal Institute of Technology, EPFL-ICP4, CH-1015, Lausanne, Switzerland. Tel.: 41-21-6933155; Fax: 41-21-6936190; E-mail: horst.vogel@icp.dc.epfl.ch.

0006-3495/99/03/1619/13 $2.00

of the ACF without detailed knowledge of the molecular processes.

THEORY

Theoretical background for FCS

In a FCS experiment, fluctuations of the fluorescence $\partial F(t)$ around the average fluorescence $\langle F \rangle$ are used to obtain information about molecular processes or molecular motions. The fluctuations of the fluorescence signal are induced by either changes in the particle number or the fluorescence quantum yield of the particles in the open probe volume, which is defined by the focal volume of a tightly focused laser. To analyze these fluctuations the ACF $G(\tau)$ of the fluorescence intensity is calculated:

$$G(\tau) = \langle F(0)F(\tau)\rangle/\langle F(\tau)\rangle^2 \tag{1}$$

with $\langle\ \rangle$ indicating a time average. The measured correlation function can now be compared to a theoretical one in order to determine the characteristic constants of the processes inducing the fluctuations.

Because in our experimental setup a laser beam with a Gaussian beam profile is used for excitation and the fluorescence is observed through a pinhole, the probe volume can be described with a Gaussian distribution in the three axes. ω_1 is defined as the distance from the optical axis and ω_2 as the distance in z-direction at which the laser has dropped by $1/e^2$, and K is defined as $K = \omega_2/\omega_1$. If only translational diffusion is observed, the ACF is (Aragon et al., 1976; Rigler et al., 1993)

$$G(\tau) = \frac{1}{N}\left(1 + \frac{\tau}{\tau_D}\right)^{-1}\left(1 + \frac{\tau}{K^2\tau_D}\right)^{-(1/2)} + DC = \frac{1}{N}g_{3d}(\tau) + DC. \tag{2}$$

The correlation time τ_D is defined as

$$\tau_D = \omega_i^2/4D. \tag{3}$$

D is the diffusion coefficient, N is the average number of light-emitting particles diffusing in the sample volume, DC is the limiting value of $G(\tau)$ for $\tau \to \infty$, which is normally 1. $g_{3d}(\tau)$ is the ACF of one particle for three-dimensional diffusion. The fit parameters are K and τ_D.

If the signal-to-noise ratio of the correlation curve was not sufficient, no reasonable values for K were obtained by fitting the experimental correlation curve. The parameter K describes the shape of the probe volume which is determined by the size of the laser focus and the pinhole. As a consequence, K should not change if the size of the focus and the pinhole are kept constant.

To obtain correct absolute particle numbers, the fluorescence background has to be considered (Koppel, 1974) and one has to correct for the inhomogeneous excitation and collection efficiency over the sample profile (Kask et al., 1997).

If higher laser intensities are used, a triplet state of the dye can be excited. This process is described by the following relation (Widengren et al., 1995, 1994)

$$G(\tau) = \frac{1}{N'}g_{3d}(\tau)[F_{Trip}e^{\tau/\tau_{Trip}} + (1 - F_{Trip})] + DC \tag{4}$$

F_{Trip} is the mole fraction of dye molecules in the triplet state, τ_{Trip} the lifetime of the triplet state, and $N' = N(1 - F_{Trip})$.

The existence of two independent diffusing components with different correlation times (τ_{D1} and τ_{D2}) changes the ACF to

$$G(\tau) = 1/N[(1 - Y)g_{3d1}(\tau) + Yg_{3d2}(\tau)] + DC \tag{5}$$

Y is the mole fraction of component 2 in the mixture, $g_{3d1}(\tau)$ and $g_{3d2}(\tau)$ the ACF for the diffusion of one particle with a correlation time τ_{D1} and τ_{D2} and thus with a diffusion coefficient D_1 and D_2, respectively, as defined in Eq. 2. This formula is correct only if both components have the same quantum yield. Taking into account different quantum yields for the general case of M components, one obtains (Thompson, 1991)

$$G(\tau) = \sum_{i=1}^{M}\alpha_i^2\langle N_i\rangle g_{3di}(\tau)\Big/\left[\sum_{i=1}^{M}\alpha_i\langle N_i\rangle^2\right]^2 + DC \tag{6}$$

where

$$g_{3di}(\tau) = (1 + 4D_i\tau/\omega_1^2)^{-1}(1 + 4D_i\tau/K^2\omega_1^2)^{-(1/2)} \tag{7}$$

and $\alpha_i = Q_i/Q_1$ where Q_i of a particle is defined as a product of absorbance, fluorescence quantum efficiency, and experimental fluorescence collection efficiency of the ith species. Taking $\alpha_i = 1$ and M = 2, Eq. 6 reduces to Eq. 5.

MATERIALS AND METHODS

Data analysis and weighting of the data

Data analysis was performed by describing the raw data with a suitable correlation function as discussed above. To fit the function to the raw data, an iterative procedure was performed with the Levenberg-Marquardt algorithm to minimize χ^2 using the software package "Igor Pro" (Wave Metrics, Lake Oswego, OR). χ^2 measures the difference between the fitted function y and the raw data y_i weighted by σ_i

$$\chi^2 = \sum[(y - y_i)/\sigma_i]^2 \tag{8}$$

summing over all data points i. σ_i is the standard deviation of the experimental point i. The estimates of the error (standard deviation) for the parameters of the fit are calculated as the square root of the diagonal matrix elements of the covariance matrix. To compare different fits the reduced $\chi_\nu^2 = \chi^2/(\nu - p)$ is calculated (ν = number of points used, p = free parameters in the fit). (For an introduction to the calculation of χ_ν^2 and other statistical parameters, see Bevington and Robinson (1992)).

When two different fit models are used, one can decide at a chosen confidence level which of the two models is more appropriate. This comparison is done by the F-test (Bevington and Robinson, 1992). Depending on the degrees of freedom and on the χ_ν^2 of the two models, the

F-distribution gives a limit for the ratio $F = \chi^2_{\nu 1}/\chi^2_{\nu 2}$ for which the two fits can be assumed to be equally well suited for the data. If this ratio is higher than the given limit, the second model will be preferred over the first. The F-distribution is tabulated (Bevington and Robinson, 1992), or is available from different software packages (such as Mathematica 3.0 (Wolfram Research, Champaign, IL).

The residuals, defined as $res = (y - y_i)/\sigma_i$, are an additional check for the goodness of the fit. They are shown for all simulations and measurements. There are several possibilities of testing whether the residuals follow trends that indicate some systematic behavior (for an overview see Straume and Johnson (1992) and references therein). Here we apply the Runs-test to quantify these trends. This test compares the expected number of runs (R, the number of series of consecutive residuals with the same sign) and the estimated variance of these expected number of runs (σ_r) with the actual number of runs (n_r). The expected number of runs can be calculated from the number of positive and negative residuals (n_p, n_n),

$$R = \frac{2n_p n_n}{n_p + n_n} + 1 \tag{9}$$

and the variance can be estimated by

$$\sigma_r^2 = \frac{2n_p n_n (2n_p n_n - n_p - n_n)}{(n_p + n_n)^2 (n_p + n_n - 1)} \tag{10}$$

The expected number of runs and the observed number of runs of the residuals can then be tested by estimating the standard normal deviate:

$$Z = \frac{n_r - R + b}{\sigma_r} \tag{11}$$

The value of b is 0.5 when testing for too few runs and -0.5 when testing for too many runs. We used a cutoff value of 2.5 standard deviations from the expected value (corresponding to a probability of about 1%) in all tests.

The standard deviation of the experimental points are calculated according to Koppel (1974, Eq. 34) using the correlation function for diffusion (see Eq. 13) instead of an exponentially decaying signal and dividing by $\langle n \rangle^4$ to allow for the normalization performed by the correlator; $\langle n \rangle$ is the average count rate per correlator channel during the measurement. This leads to the following expression for the standard deviation of the correlation signal $G(\tau)$:

$$\sigma^2(G(\tau)) = \frac{1}{M}\frac{1}{N^2}\left\{\frac{(1 + g^2(\Delta\tau))(1 + g^2(\tau))}{1 - g^2(\Delta\tau)} + 2mg^2(\tau)\right\} + \frac{1}{M}\left\{\frac{2(1 + g^2(\tau))}{N\langle n \rangle} + \frac{1}{\langle n \rangle^2}\left(1 + \frac{g(\tau)}{N}\right)\right\} \tag{12}$$

$\Delta\tau$ is the channel width of the correlator, $M = t/\Delta\tau$ the number of counting intervals, t the measuring time of the experiment, N the average number of particles, $m = \tau/\Delta\tau$. The calculation is based on the signal for simple two-dimensional diffusion,

$$g(\tau) = \left(1 + \frac{\tau}{\tau_D}\right)^{-1} \tag{13}$$

This estimation of the standard deviation is only an approximation of the real standard deviation but should be qualititatively correct (Koppel, 1974). For a correct calculation of the standard deviation it has to be calculated from the original intensity signal which is not available from presently available hardware correlators (Rigler and Widengren, Quart. Rev. Biophys., submitted).

Estimation of the error of the correlation time

To estimate the error of measuring the correlation time, the formula for the absolute error for $\Gamma = 1/\tau_D$ calculated by Koppel (1974, Eq. 51) was used:

$$\frac{\sigma(\tau_D)}{\tau_D} = \frac{\sigma(\Gamma)}{\Gamma} = 2^{3/2}\frac{\Gamma N}{\bar{n}}(\Gamma t)^{-(1/2)} \tag{14}$$

where $\bar{n}$ is the average count rate per second.

This formula was calculated for an exponential correlation function but it can be used as a first approximation with which to compare the simulations. It should be noted, furthermore, that this equation was derived for the low-counting-rate limit (i.e., count rate per particle and per channel much smaller than 1, $\bar{n}\,\Delta\tau/N \ll 1$).

Description of the simulations

For the simulations, first, an ideal autocorrelation curve according to one of two theoretical models (Eq. 2 or 5) was calculated: one for three-dimensional diffusion of one molecular species (Eq. 2); the second for a sample composed of two sorts of particles distinguished by two correlation times (Eq. 5) but identical count rate per particle.

To compare the simulations with experimental data, the scaling of the correlation time axis was chosen to be identical with that of the correlator used (a multiple τ correlator with a semilogarithmic time scale doubling the channel width after each 8 channels; 200 channels were used altogether).

In all fits the correlation time τ_D (Eq. 2) is calculated. To relate τ_D to the diffusion coefficient of the molecule, the radius ω_1 of the probe volume must be known. Under the experimental conditions used ($\omega_1 = 0.25\ \mu m$) the diffusion coefficient of Rho 6G ($D = 2.8 \times 10^{-6}\ cm^2/s$) corresponds to $\tau_D = 56\ \mu s$ (see experiments).

Noise was added to the model functions simulating the statistical fluctuations of data around a mean in a real experiment. This noise was chosen to be described by the standard deviation calculated for FCS experiments (Koppel, 1974, Eq. 9). This noise is a function of the measuring time t, the average number of particles N in the focal volume, and the average count rate per channel $\langle n \rangle$ (not to be confused with the average count rate per second $\bar{n}$, $\langle n \rangle = \bar{n}\,\Delta\tau$, $\Delta\tau$ is the channel width). For all simulations the time was set to $t = 300$ s and the number of particles to $N = 1$. The average count rate $\bar{n}$ was chosen to be 15 kHz, as observed experimentally for Rhodamine at medium laser power (in the range of μW). A second case with $\bar{n} = 1$ kHz was analyzed. This is a very low signal as observed for example for the widely used fluorescence label NBD (N-[7-Nitrobenz-2-oxa1,3-diazol-4-yl]). Random values with a Gaussian distribution and a root mean square equal to this standard deviation were added to each point of the simulated curve.

For each situation (set of parameters) ten simulations, each with a different noise, were produced and fitted as described under data analysis. The final result of the fit is the average of these ten simulations with the standard deviation calculated for the distribution of the ten values. (This standard deviation was normally the same to within 20% of the estimated error for one fit, the root of the diagonal matrix elements of the covariance matrix of the fit). The relative errors were calculated in two ways. When the model appropriate for the situation (i.e., one-component fit for a one-component simulated curve, and so on) was used, the relative error was determined with the input values for the simulation. When the inappropriate model (i.e., one-component fit for a two-component situation, and vice versa) was used, the relative error was determined from the standard deviation and the mean value of the fitted parameter.

To discuss the problem of time resolution, the simulations representing two-particle diffusion were evaluated in two different ways using either the one-particle model (parameters: N, τ, DC), or the two-particle model (parameters: N, τ_{D1}, τ_{D2}, Y, DC). Both evaluations were compared and two different values of χ^2_ν and of the residuals were used to discuss which evaluation is appropriate for this particular case.

In our simulations we used 200 data points and two models with three and five parameters, respectively. For a confidence level of 95% the

distribution yields a value of F = 1.266; for a confidence level of 99%, F = 1.396.

Experimental setup for FCS

The fluorescence correlation spectrometer is centered around an inverted Axiovert 100 TV microscope (Carl Zeiss, Oberkochen, Germany). It consists of a Coherent INNOVA Sabre Ar^+-Laser (Coherent, Santa Clara, CA) with an output beamwaist of 3 mm. The 514-nm line was used for excitation of the fluorophores. The laser beam is expanded to 6 mm by a Keplerian beam expansion and is then directly reflected by a dichroic mirror (FT540, Omega, Brattleboro, VT) into the microscope objective (63× C-Apochromat, NA 1.2, water immersion with coverslip correction for a thickness between 0.16–0.18 μm, Carl Zeiss). The beam expansion ensures that the back aperture of the microscope objective is fully illuminated, thus providing a tightly focused laser beam. The fluorescence signal of the sample is collected with the same objective and passes through a band pass filter (565DF72, Omega) to reduce the background signal. A pinhole, 50 μm in diameter, is installed in an image plane of the microscope to discriminate against out-of-focus signals. The collected fluorescence light is then focused onto an avalanche photo diode (SPCM-100, EG&G, Princeton, NJ). The electrical signal is fed into a hardware correlator (ALV-5000, ALV-GmbH, Langen, Germany) and the ACFs are calculated using a semilogarithmic time scale.

The power of the laser beam entering the microscope was set to 80 μW for all experiments. This power level creates reasonably high fluorescence signals per molecule, but is still low enough to keep photobleaching negligible. The actual power in the sample volume is lower due to losses at lenses, beam splitter, and dichroic mirror. The actual laser intensity in the focal volume was not measured. As sample cells we used eight-well cover glass chambers (Nunc, Wiesbaden, Germany).

The beamwaist radius of the focused laser beam was determined to be 0.25 μm by measuring the translational diffusion of Rho 6G in water, assuming a diffusion coefficient of $D = 2.8\ 10^{-6}$ cm^2/s (Rigler et al., 1993). This value is close to the theoretical expected beamwaist radius of 0.23 μm calculated by Gaussian optics.

Chemicals

For the single- and two-particle system measurements the following fluorophores and fluorescently labeled molecules were used: Rhodamine 6G (Molecular Probes, Leiden, The Netherlands) and bovine tetramethylrhodamine isothiocyanate albumin (TRITC-albumin/Rho-BSA, Sigma, Buchs, Switzerland). One molecule of albumin contains one tetramethyl rhodamine molecule on average. All chemicals were dissolved in deionized water (Nanopure, Skan AG, Basel, Switzerland). Nonlabeled bovine serum albumin (BSA) was obtained from Sigma (Sigma, St. Louis, MO). HEPES was from Fluka Chemie AG (Buchs, Switzerland).

Measurement principle

To suppress nonspecific protein binding, the cover glass wells were coated with nonfluorescent BSA before starting the measurements. This was achieved by incubating the wells with a solution of 1 mg BSA/ml in HEPES buffer for 10 min exchanging the solution, and repeating this procedure twice. The wells were rinsed with pure water after BSA incubation.

The cover glass thickness correction of the microscope objective was adjusted to yield the smallest focus possible, i.e., the smallest amount of molecules per observation volume of a Rho 6G solution.

Stock solutions of Rho 6G and Rho-BSA in water were prepared and diluted by water to the final desired concentration for FCS measurements. The molar fraction of Rho-BSA as defined by this procedure is denoted as Y_1. No buffer was used to minimize the autofluorescence signal of the solvent with respect to the solute molecules. Typically 100 μl of the solutions were injected into the sample chambers. Each sample was measured 10 times with a duration of 120 s for each measurement. ACFs were calculated online. Count rates were typically between 45 and 420 kHz; the background was smaller than 2 kHz. The number of experiments, their duration, and the high count rates are necessary for good statistics.

The resulting ACFs were fitted to three different models. The first model is a single-component model (Eq. 4) which assumes only one fluorescent component in the solution including a possible triplet state (fixed parameter: K; free parameters: N, τ_D, F_{trip}, τ_{trip}, DC). The second model (Eq. 6) assumes two components simultaneously in solution plus one triplet state. The correlation times for Rho 6G (τ_{Rho}) and Rho-BSA (τ_{BSA}), K, as well as the value for $\alpha = Q_{BSA}/Q_{Rho}$, as defined above in Theory, were fixed and a parameter for the molar fraction of Rho BSA, Y_2, is introduced (fixed parameters: τ_{Rho}, τ_{BSA}, K, α; free parameters: N, Y_2, F_{trip}, τ_{trip}, DC). The third model (Eqs. 4 and 6 modified with a second triplet factor) describes two particles in solution as well as two triplet states, one for each component. The parameter for the molar fraction of Rho-BSA is Y_3 (fixed parameters: τ_{Rho}, τ_{BSA}, K, τ_{trip1}, τ_{trip2}, α; free parameters: N, Y_3, F_{trip1}, F_{trip2}, DC). The triplets are necessary in all three models to fit the experimental results accurately at times that are short compared to the diffusion correlation times of the molecules. All fixed parameters were set to the experimental values given in the next paragraph.

In our measurements we collected 125 data points. To decide between the single-component model and either the two-component model with one triplet or the two-component model with two triplets, we used the F-test. At a confidence level of 99%, $F = 1.541$ for the ratio of the χ^2_ν for the one-component model and the two-component model with one triplet. This value is slightly higher ($F = 1.544$) at the same confidence level for the one-component model, compared to the two-component model with two triplets.

RESULTS

Results of the simulations

For clarity, only χ^2 for the different conditions of the simulations are shown. The tables with all parameters and errors are published elsewhere (Meseth, 1996, available on the web at *http://icpsg3.epfl.ch/Lit/PhDtheses/thesisMeseth/*).

Simulation of one diffusing component

In a first series of simulations, the model of one-particle diffusion in solution was tested using Eq. 2. The simulation of the correlation curve and its standard deviation for one-particle diffusion with a correlation time of 1 ms are shown in Fig. 1. The curves resemble quite well the behavior of the autocorrelation curve of a real experiment.

A series of simulations with different correlation times and two different count rates (1 kHz and 15 kHz per particle) were performed. In all the cases the particle number and the parameter DC are fitted with better than 1% accuracy. The errors of the correlation times are shown in Fig. 2 (*diamonds*, 15 kHz per particle, *triangles*, 1 kHz per particle). In the same figure, the relative errors of the correlation time as calculated according to the theoretical estimate (Eq. 14) are also shown (solid lines). They were calculated for different count rates per particle (15, 7.5, 1, and 0.1 kHz). For correlation times shorter than about 0.1 ms, the error estimated with the simulation and the theoretical estimation are in the same range and decrease with τ_D. On increasing τ_D above 0.1 ms, the low-counting rate assumption for the theoretical estimate (Eq. 14) is no longer

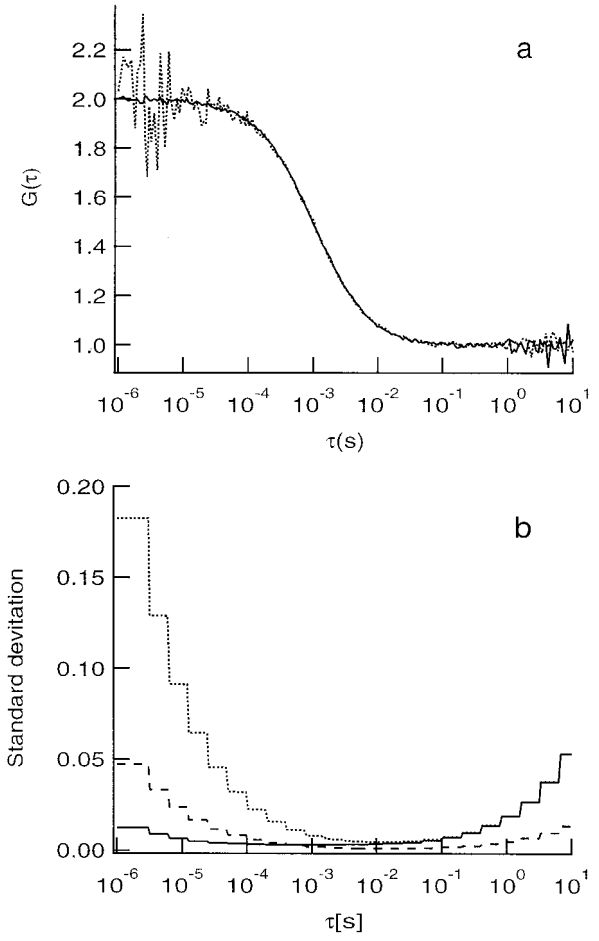

FIGURE 1 (*a*) Simulated autocorrelation curves for three-dimensional diffusion with an average of one particle in the sample volume and a diffusion time of 1 ms. The statistical noise was calculated for the case of t = 300 s measuring time with an average count rate per particle of 15 kHz (*solid line*) or 1 kHz (*dotted curve*). (*b*) Corresponding standard deviations (according to Eq. 12) used to simulate the curves. In addition, the simulated standard deviation for a measurement at 1 kHz count rate and t = 4500 s (*dashed line*) is shown.

fulfilled. Above 1 ms, the relative errors of the simulations stay more or less constant and are better than 1%.

Simulation of two diffusing components

The autocorrelation curves for two diffusing components in solution were simulated using Eq. 5. For simulation, the curves were fitted by both the one- and the two-particle model.

Data were simulated for the two cases in which the fraction of the second component, factor Y in Eq. 5, is either 0.5 or 0.1. Assuming identical count rates per particle for the two components, this factor Y corresponds to the real mole fraction of component 2. One should keep in mind that if one component has a higher fluorescence intensity, e.g., in an aggregate with more than one dye, this has a strong influence on the result. According to Eq. 6, the fraction of each component depends on the square of the ratio of the

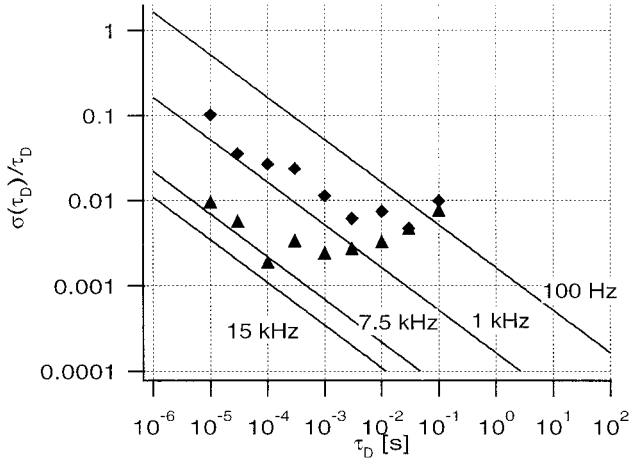

FIGURE 2 Relative error for the measurement of the diffusion time as calculated with Eq. 11 for an experiment of t = 300 s, $N = 1$, and different count rates per particle as indicated in the graph. The results from simulations are shown for a signal of 15 kHz per particle ▲ and 1 kHz per particle ◆. In both cases the simulation time was t = 300 s.

corresponding count rates α. Thus a small error in α will have a significant influence on the result.

Two sets of simulations will be considered in the following. In the first situation, one correlation time $\tau_1 = 1$ ms was always kept constant while τ_2 was changed. This is shown in Fig. 3 for two different distributions of particles, Y = 0.5 and Y = 0.1. The results showing how χ^2_ν changes with respect to the ratio τ_2/τ_1 between the correlation times, are depicted in Fig. 3.

In a second set of simulations the ratio τ_2/τ_1 was kept constant ($\tau_2 = 3 \times \tau_1$). The results are shown in Fig. 4.

Results of the experiments

The correlation time of Rho 6G in water was measured by 10 different experiments, yielding a value of 57.7 ± 0.6 μs with a count rate per particle of 30 kHz. Using a diffusion coefficient for Rho 6G of D = 2.8 10^{-6} cm^2/s (Rigler et al., 1993) a beamwaist radius of the focused laser beam of 0.25 μm (Eq. 3) is calculated. The value of K was determined by these measurements to be 5. In all subsequent fits this value was held constant because it should not change within one experimental setup, as discussed above in Theory. The triplet correlation time of Rho 6G was determined to be 8 ± 2 μs.

The correlation time of Rho-BSA was measured in the same manner to be 330 ± 5 μs with a count rate of 12 kHz per particle, yielding a diffusion coefficient of 4.9 ± 0.1 10^{-7} cm^2/s (Eq. 3). The triplet correlation time was 32 ± 2 μs. The value α for Rho 6G and Rho-BSA was calculated as the ratio of the counts per molecule at the same excitation intensity for the two different fluorophores and yielded a value of $\alpha = 0.4$.

The results for the series of experiments of increasing Rho-BSA molar fraction are shown in Table 1. For the one-component model we found a monotonously rising

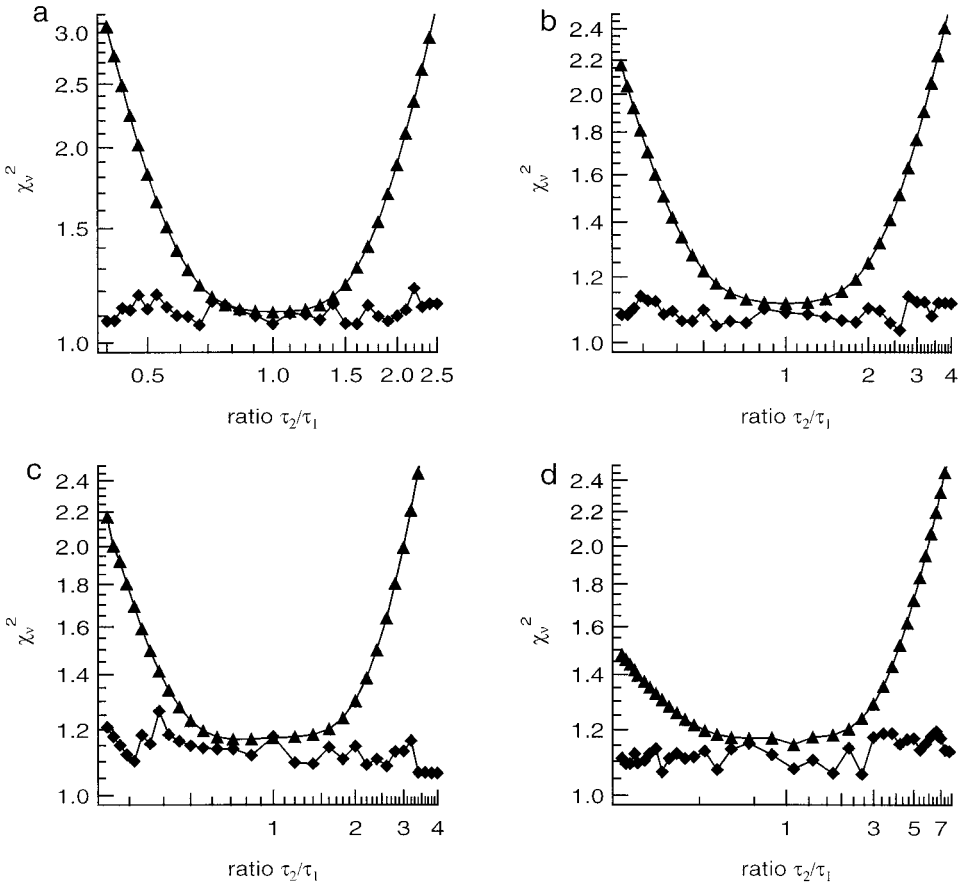

FIGURE 3 Autocorrelation curves simulated for two diffusing components with different ratios of τ_2/τ_1 and $\tau_1 = 1$ ms. Fits using the one-component model (triangles) and two-component model ◆ were performed and the χ_ν^2 were plotted. In (*a*) and (*b*) a count rate of 15 kHz was assumed, in (*c*) and (*d*) one of 1 kHz. The fraction of particles moving with τ_2 is Y = 0.5 in (*a*) and (*c*) and Y = 0.1 in (*b*) and (*d*).

correlation time from 55.4 to 105.4 μs with an increase of the expected fraction of Rho-BSA (Y_1) from 0.12 to 0.93 of the total fluorescent molecule concentration. The χ_ν^2 value ($\chi_{\nu 1}^2$) ranges between 0.72 and 1.51 for this model. For fractions of Rho-BSA smaller than 0.53 as determined by the two-particle fits (Y_2 and Y_3), the one-particle fit yields $\chi_{\nu 1}^2 \leq 1.02$. For the mixed solutions the triplet correlation time was fitted between 11 and 27 μs.

In the second model describing two components and one triplet state, the correlation times for Rho 6G and Rho-BSA from the previous measurements were fixed because otherwise the fits were not properly terminated. The quantum yield ratio between the two fluorescent components was fixed to the previously determined value of 0.4. The fitted fraction of Rho-BSA, Y_2, rises from 0.34 to 0.65 compared to the expected fraction, which ranges from 0.12 to 0.93. The χ_ν^2 value ($\chi_{\nu 2}^2$) ranges from 0.72 to 1.13. The triplet correlation time ranged between 10 and 20 μs.

The third model (two components and two triplet states) yields values for the fraction of Rho-BSA, Y_3, in solution very similar to the corresponding values of Y_2 in the second model. But the values for χ_ν^2 are smaller than the values obtained by the second model and range between 0.6 and 0.88 ($\chi_{\nu 3}^2$). The results are given in Table 1.

TABLE 1 Fits to the experimental results

	1-particle, 1 triplet		2-particle, 1 triplet		2-particle, 2 triplets	
Value of Y_1	τ_D [μs]	$\chi_{\nu 1}^2$	Y_2	$\chi_{\nu 2}^2$	Y_3	$\chi_{\nu 3}^2$
0.12	55.4 ± 0.9	0.72 ± 0.09	0.35 ± 0.01	0.94 ± 0.13	0.38 ± 0.01	0.60 ± 0.09
0.21	59.9 ± 1.8	0.84 ± 0.16	0.40 ± 0.02	0.91 ± 0.16	0.43 ± 0.02	0.61 ± 0.13
0.37	64.0 ± 1.2	0.86 ± 0.15	0.46 ± 0.01	0.72 ± 0.10	0.48 ± 0.01	0.62 ± 0.10
0.70	67.6 ± 2.2	1.02 ± 0.12	0.47 ± 0.02	0.92 ± 0.12	0.50 ± 0.02	0.60 ± 0.08
0.54	71.6 ± 3.0	1.0 ± 0.12	0.52 ± 0.02	0.72 ± 0.08	0.53 ± 0.02	0.60 ± 0.06
0.64	79.2 ± 2.8	1.24 ± 0.28	0.56 ± 0.02	0.89 ± 0.22	0.44 ± 0.02	0.62 ± 0.13
0.78	99.0 ± 7.9	1.51 ± 0.21	0.64 ± 0.03	0.99 ± 0.17	0.66 ± 0.03	0.82 ± 0.14
0.93	105.4 ± 6.9	1.41 ± 0.21	0.65 ± 0.03	1.13 ± 0.19	0.67 ± 0.02	0.88 ± 0.16

Y_1 is the expected fraction of Rho-BSA in solution as determined by the concentrations of the stock solutions before mixture. τ_D is the correlation time for the one-particle fit. Y_2 and Y_3 are the molar fractions of Rho-BSA found by fitting the experimental results with model 2 (two-particle fit, one triplet) and model 3 (two-particle fit, two triplets), respectively. The values $\chi_{\nu 1}^2$, $\chi_{\nu 2}^2$, and $\chi_{\nu 3}^2$ measure the goodness of the fit for the three different models.

Values for DC were usually 1 with deviations smaller than 1%. The fractions of molecules in the triplet state obtained by the fit were about 0.1.

All attempts to fit the experimental correlation curves with models failed where only the parameter K of the measurement setup is fixed and all other parameters are free. Either the fits were not properly terminated, i.e., the model diverged from the raw data, or the results obtained were not sound (e.g., fractions Y or $F_{trip} < 0$).

DISCUSSION

When calculating the diffusion coefficient there are several sources of errors. The diffusion coefficient of an unknown substance can only be calculated by comparison to an experiment with a known substance (normally Rho 6G). Thus, the error of the diffusion coefficient accumulates the error of both experiments.

The absolute value of the correlation time is very sensible to alignment and thickness of the coverglass (if not measured directly in the solution). The diameter of the focus and thus the correlation time increases by a factor of two when there is a mismatch of only 20 μm between the thickness of the coverglass and the thickness for which the objective is corrected (Keller, 1995).

All fits to the experimental data are performed using Eq. 12. This equation is qualitatively correct but overestimates the variance of the experiments. This is clearly demonstrated by the fact that $\chi^2_\nu < 1$ for most experiments (see Table 1). This indicates that the assumed variance is higher than the experimental variance resulting in the underestimation of χ^2_ν.

The simulations rely on the same model for the calculation of the variance. Because the variance of the experiments is overestimated, the simulations represent a worst-case scenario which should nevertheless be qualitatively correct.

Simulation of one-component diffusion

The simulations show that the experimental error of the correlation time should be below 1% for a count rate of 15 kHz per particle. In our experiments the error in the correlation time was about 1%.

The standard deviation (σ^2) of the signal as shown in the lower part of Fig. 1 depends strongly on the count rate per particle in the fast time range. For example, increasing the signal from 1 to 15 kHz reduces σ^2 from about 0.18 (dotted line) to 0.01 (*solid line*) at a correlation time of 1 μs. For longer correlation times ($\tau > 0.1$ s), σ^2 becomes independent of the signal intensity. The only way to reduce the experimental error in this time region is to increase the total measuring time. This is shown with the dashed curve in Fig. 1 where a signal of 1 kHz and a measuring time of 4500 s were assumed. The steps in the error function of Fig. 1 *b* are due to the changes in the channel width of the correlator.

Simulations of two-component diffusion

Three different aspects of the simulations will be discussed. First, it will be investigated which conditions have to be fulfilled to justify the evaluation of an experiment with the two-particle model. Next, the errors of the different parameters, e.g., correlation time, fraction, or particle number, are considered. Finally, the simulations are compared to the experiments and the influence of the count rate per particle is discussed.

Evaluation with the two-particle model

The two-particle model normally fits each experiment better than the one-particle model because it introduces more fit parameters. To determine whether it is justifiable to use more parameters in the fit, two criteria can be applied, χ^2_ν and the residuals of the fit.

To compare the values of the χ^2_ν, the F-test was performed as described above in Theory. The model with more fit parameters was assumed to be justified when the ratio of χ^2_ν of the two models exceeded the value $F = 1.396$ determined by the F-distribution at a confidence level of 99% for the corresponding degrees of freedom (200 data points, three and five parameters for the one- and two-particle models, respectively). According to this criterion, the resolution of FCS for the different situations (count rate per particle and Y, the fraction of component 2) is as follows: a factor of 1.6 in the correlation time is sufficient to distinguish particles with identical probability of occurrence (Y = 0.5) and a count rate of 15 kHz per particle (Fig. 3 *a*). If there are only 10% of the particles of the second size (Y = 0.1), the correlation times must differ by a factor of about 2.6. Given a lower signal per particle (1 kHz), a difference in the correlation times of more than a factor of 3 is required for an equal distribution (Y = 0.5). In the case of Y = 0.1, the minor component cannot be resolved if the factor between the diffusion times is smaller than 10 (for example see Fig. 6, the fit of one-particle diffusion to the simulated data of two-particle diffusion with $\tau_2/\tau_1 = 0.1$). Only if τ_2 is >5 ms, i.e., slower than τ_1 by a factor of 5, can both particles be distinguished. For $\tau_2 < \tau_1$ the particles cannot be distinguished because the relative error in the measured τ_D becomes too high (see Fig. 2), making a proper fit impossible.

Consider the simulations where the ratio between τ_2 and τ_1 was kept constant. As shown in Fig. 4 with $\tau_2/\tau_1 = 3$, it is clear that a discrimination is possible for correlation times τ_D between 0.01 and 100 ms; below and above this time window, no distinction is possible. For a signal of 1 kHz the same effect is observed but the discrimination is worse.

Another criterion to justify the application of the two-particle model comes from a statistical analysis of the residuals (the difference between the fit and the data to be fitted, divided by the square of the standard deviation). If the residuals are not randomly distributed around zero, the fit is not reliable. We used the Runs-test to determine if there are trends in the residuals (see Theory) and we used a

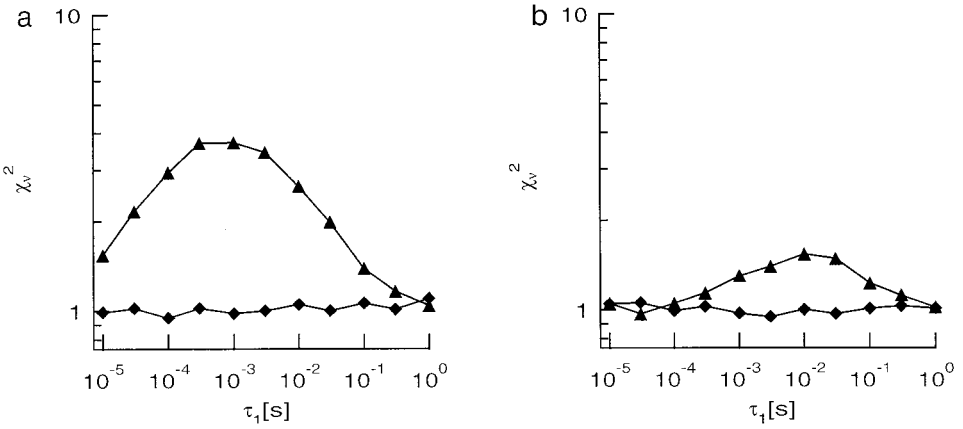

FIGURE 4 Autocorrelation curves simulated for two diffusing components with $\tau_2 = 3\ \tau_1$, τ_1 as shown on abscissa. Fits to a model for one particle ▲ and two particles ◆ were performed and the χ_ν^2 were plotted as a function of τ. In (*a*) a count rate of 15 kHz was assumed, in (*b*) one of 1 kHz. The fraction of particles moving with τ_2 is 0.5.

cutoff value of 2.5 standard deviations. For all two-particle models, the deviation of the observed runs from the number of expected runs was around 1, indicating that no systematic trends are present in the behavior of the residuals. For the one-particle model, the Runs-test yielded the following: The factor between τ_1 and τ_2 must be at least 1.7 (count rate 15 kHz, Y = 0.5) to determine that the one-particle model is not appropriate (the number of actual runs deviates by more than 2.5 standard deviations from the expected number of runs). For the same count rate (15 kHz) but a lower mole fraction of the second molecule (Y = 0.1), the factor has to be at least 2.4. For lower count rates, the factor between τ_1 and τ_2 must be at least 2.8 (count rate 1 kHz, Y = 0.5) and 4.6 (count rate 1 kHz, Y = 0.1, $\tau_1 < \tau_2$) and 8 (count rate 1 kHz, Y = 0.1, $\tau_1 > \tau_2$). The results of the Runs-test are in very good agreement with the results of the F-test used to compare the χ_ν^2 values of the two models. Both tests were performed at a confidence level of 99%.

The behavior of the residuals is illustrated in Figs. 5 and 6. In Fig. 5 it seems justified to use the two-particle fit; the residuals of the one-particle fit (res a) are not evenly distributed in the time range of τ_D as indicated by the arrows. In Fig. 6 the one-particle fit describes the curve as well as the fit with two particles; here it is not justified to use the two-particle fit. However, this criterion is sometimes difficult to apply in a real experiment. The fits to experimental data often show a slight bend of the residual around τ_D as observed with the wrong fit (compare res a in Figs. 5 and 7).

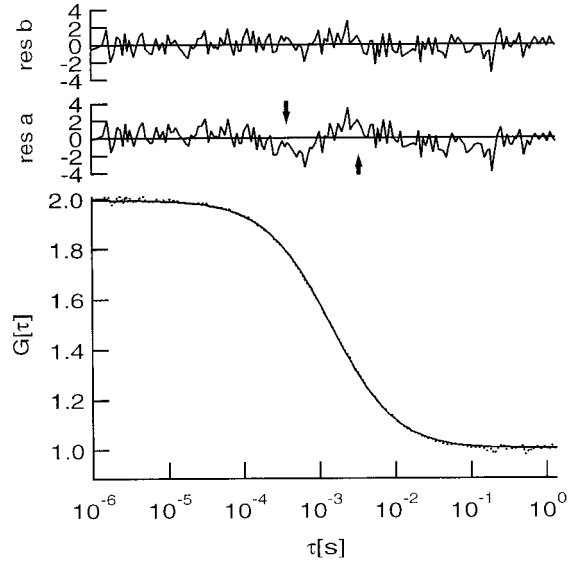

FIGURE 5 Simulated correlation curve for two particles (*dotted curve*, 15 kHz count rate, t = 300 s, $N = 1$, $\tau_1 = 1$ ms, $\tau_2 = 2$ ms, Y = 0.5) with a fit for one-particle diffusion (*solid line*, $\tau_1 = 1.4 \pm 0.005$ ms, $\chi_\nu^2 = 1.5$, residuals shown as "res a"), and the residuals for a fit with two-particle diffusion (residuals shown as "res b": $\tau_1 = 1.1 \pm$ ms, $\tau_2 = 2.2 \pm 0.6$ ms, Y = 0.4 ± 0.3, $\chi_\nu^2 = 0.8$). This is the limiting case for which the two-component fit is justified. $\chi_\nu^2 \geq 1.5$ and the residuals are not equally distributed around zero (*arrows*).

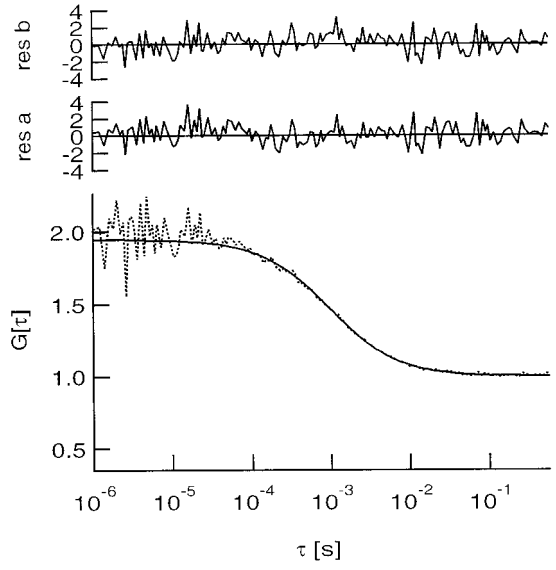

FIGURE 6 Autocorrelation curve simulated with noise for a signal of 1 kHz count rate (*dotted curve*, t = 300 s, $\tau_1 = 1$ ms, $\tau_2 = 0.1$ ms, Y = 0.1). The fit with one-component diffusion (*straight line*, $\tau_1 = 0.96 \pm 0.01$ ms, $\chi_\nu^2 = 1.11$) is shown. The residuals of the fit are shown as "res a." The residuals of a fit with two components are shown as "res b" ($\tau_1 = 0.97 \pm 0.03$ ms, $\tau_2 = 0.02 \pm 0.02$ ms, Y = 0.13 ± 0.03, $\chi_\nu^2 = 0.9$). There is no justification for choosing the two-component model.

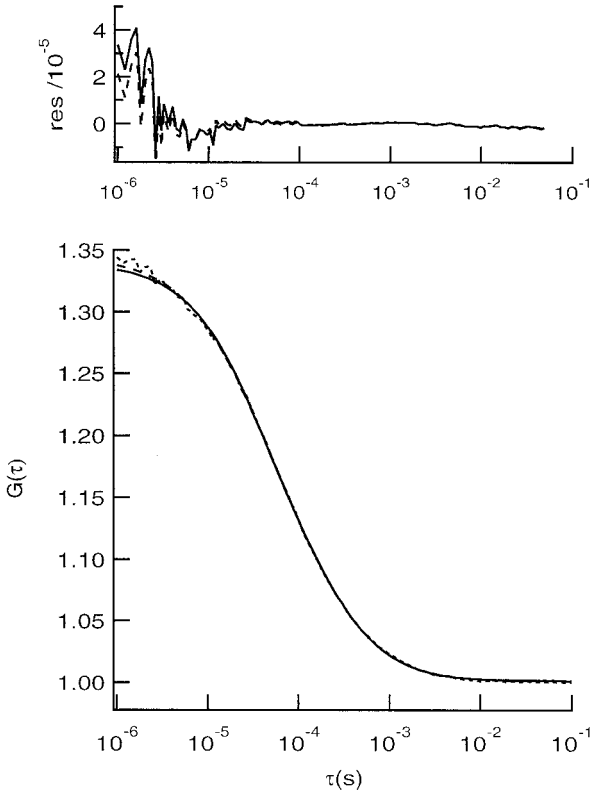

FIGURE 7 Experimental autocorrelation curve of a mixture of Rho 6G and Rho-BSA (*dotted line*, Y = 0.68). The one-particle fit is shown as a solid line and its residuals are shown as "res a" ($N = 2.95 \pm 0.01$, $\tau_1 = 104.0 \pm 2.0$ μs, $F_{Trip} = 0.24 \pm 0.01$, $\tau_{Trip} = 28.0 \pm 10$ μs, $\chi^2_\nu = 1.54$). The two-particle fit is shown as a dashed line; its residuals are shown as "res b" ($N = 3.56 \pm 0.01$, $\tau_1 = 58.0$ μs (fix), $\tau_2 = 329.0$ μs (fix), $Y = 0.66 \pm 0.01$, $F_{Trip} = 0.09 \pm 0.004$, $\tau_{Trip} = 15.0 \pm 1$ μs, $\chi^2_\nu = 1.1$). The errors given are the estimate of the fit to one experiment.

This makes it difficult to judge whether one is observing a mixture of different particle sizes or some other effects.

This shows that the presence of two different particle sizes can be distinguished clearly only if the correlation times differ by a factor of 1.6 to 8, depending on the count rate of the signal and the fraction of the second component present. Thus, the particles must have a mass difference of a factor of 4 to 500, because the relative molecular mass is proportional to D^{-3}. In the case of smaller mass differences one obtains an apparent good fit using the one-particle model; however, the diffusion time obtained is the mean of the two diffusion times. This is evident, e.g., in Fig. 5, where the simulation was calculated for the correlation times $\tau_1 = 1$ ms and $\tau_2 = 2$ ms but a good fit was obtained by using a correlation time of $\tau_D = 1.4$ ms.

Errors of different parameters

A point of interest is the error of each parameter in the fit. The particle number is, in principle, fitted with a relative error below 0.02 except when the signal is weak (1 kHz) and the correlation time is fast ($\tau_D < 50$ μs).

If two-particle diffusion is fitted with a one-particle diffusion model, the measured correlation time is an average of the real correlation times. The relative error of the one-particle correlation time is lower than the error of the correlation times when applying the correct model (see Figs. 5 and 6).

If the correct model with two-particle diffusion can be applied, the correlation time of the major component always has the smaller error. In the case where the second component is only present with Y = 0.1, the relative error of the correlation time of the second component is up to 0.3.

The ratio between the two components can be measured with a relative error of less than 0.06 for Y = 0.5 and a signal of 15 kHz count rate: for a lower signal the error was slightly higher. If the fraction of one particle is lower (Y = 0.1), the error is bigger than 0.1.

Influence of the count rate per particle

The correct evaluation of the count rate per particle is also essential for the correct determination of ratios between two diffusing components. This can sometimes be difficult. If, e.g., a binding reaction is measured, the quantum yield of the dye can be different in the bound and unbound states, or there may exist more than one bound state with different numbers of binding partners. The ratio of the count rates per particle observed for each fraction enters as α in the evaluation (see Eq. 6). Unfortunately, the measurement depends on the square of α, so that small errors in α result in a large final error (see e.g. Rauer et al., 1996).

Discussion of the experimental results

The diffusion coefficients of Rho 6G and of Rho-BSA in water were determined by FCS measurements. Mixtures of these stock solutions were prepared in different molar ratios and the capability of FCS to detect whether one or two components are present in the sample was tested. The possibility of distinguishing between the two cases depends on the molar ratio between the components.

For the single-component solutions, the relative errors were 1% and 1.6% for Rho 6G and Rho-BSA, respectively. Such values are expected from the simulations. The resulting diffusion coefficient for Rho-BSA of $(4.9 \pm 0.1)\ 10^{-7}$ cm^2/s is slightly lower than the value found in literature ($5.9\ 10^{-7}$ cm^2/s, (Tanford, 1961).

For a solution composed of two components, three different models were used to fit the experimental curves. The one-component fit shows an increase in the calculated correlation time with the increasing fraction of Rho-BSA in solution, which can be attributed to the characteristics of the fit model. Only one correlation time is available in this model, whereas the sample actually contains two fluorophores with significantly different correlation times. Therefore, the least squares fit delivers a value which is the average of these correlation times weighted by their relative

fractions in solution and their relative quantum yield. An increase of the correlation time in the framework of this model can be an indication of aggregation or binding. Furthermore, because the one-component model yields values of $\chi^2_{\nu 1} \leq 1.02$ for fractions of Rho-BSA smaller than 0.5 (Y_2), there is no evidence in these cases that the model is inappropriate to these particular experimental situations.

The second model results in values for $\chi^2_{\nu 2}$ close to 1 for all measurements. This indicates that the fits satisfactorily predict the experimental ACF within the standard error of the measurement. The fraction of Rho-BSA of the total fluorescent molecules in solution was determined from the concentrations of the mixed stock solutions and their mixing ratio (Y_1), as well as from the two-component fits with one and two triplets (Y_2 and Y_3, respectively). From these values, it is clear that the fitted fractions of Rho-BSA and the fraction determined by the mixing of the stock solutions are at odds. This is probably due to the fact that, even after coating our cover glasses with BSA, we still lose some of the Rho 6G and the Rho-BSA from the solution by interactions with the glass surface. This is already indicated by the fluorescence intensity seen when focusing on the surface of the coverglass, which is significantly higher than the intensity from the back-scattered light that is filtered in front of the detector. Even in the best case, the deviation of Y_1 from Y_2 is on the order of 0.2. Therefore, we assume that the FCS-measured mole fractions reflect the actual concentrations in solution. This assumption is supported by the fact that the number of particles per sample volume N does not change within the measurement time and has a very low relative error as given in the fit routines. In all fits we kept the diffusion times constant. In the two-component model with two triplets, even the triplet lifetimes were set to the experimentally determined values, so that only the fraction of the triplets and the fraction of Rho-BSA were allowed to vary. Note that the situation is different if binding measurements are performed; in such a case, one should link all fits, assuming a single K_d value. Performing such global fits might then improve considerably the ability to distinguish between two fractions in dependence of concentration over the whole range of concentrations (Beechem, 1992).

Closely related to this problem is the measurement of the ratio $\alpha = Q_{BSA}/Q_{Rho}$ for the combination of fluorophores. As can be seen by Eq. 6, the fractions Y_2 and Y_3 of the components are weighted with the square of their relative count rates per particle. Therefore the value of α must be determined to a high accuracy to guarantee a correct interpretation of the fractions in solution. This problem was solved here by measuring the photons per molecule per time interval for a fixed laser power for both fluorophores separately. However, if only one fluorophore is used to observe binding or aggregation, one would need one-component solutions of ligand-receptor complexes or aggregates and their corresponding components before binding or aggregation, respectively. Because these are usually difficult to produce, other methods have to be used to determine the relative quantum yields. A good example is the static fluorescence titration (SFT) technique used in the study of the binding of α-bungarotoxin to the acetylcholine receptor (Rauer et al., 1996).

The triplet correlation time for models 1 and 2 range between 10 and 27 μs and reflect a weighted average of the triplet correlation times for Rho 6G and Rho-BSA. The average depends on the triplet population of the two fluorophores and on their contribution to the fluorescence signal. Long triplet correlation times in this range were already found for fluorescein (Song et al., 1997).

To test for systematic deviations in the residuals we performed a Runs-test for every fit. For the one-component model, the averaged value of Z was 6. For the two-component model with one triplet state, this value decreased to 5. For the two-component model the value of Z was between 3 and 4. This clearly shows a trend where for the more appropriate models, we have smaller deviations between the *actual* number of runs and the *expected* number of runs. Nonetheless, all Z values are beyond the cutoff value of 2.5 standard deviations, indicating that we have fewer runs than expected ($n_R - R < 0$ for all fits) (see Eq. 11). This might be due to the deviations between the fit functions and the experimental data at very short times ($\tau < 10^{-6}$ s, see Fig. 7). In this context, there are several other tests that can be performed, such as an autocorrelation of the residuals (for more detailed information see Straume et al., 1992).

A comparison of the χ^2_ν of the first and second model by the F-test shows that a ratio of $\chi^2_{\nu 1}/\chi^2_{\nu 2} > 1.541$ appears only for measurements with $Y > 0.6$ (F value for models with 125 data points and 6 and 9 parameters respectively, at a confidence level of 99%). Therefore, we conclude that only at high mole fractions Y is it possible to determine with this model, without detailed knowledge of the molecules in solution, whether there are one or two components present.

For model 3, the prospects are better. A ratio $\chi^2_{\nu 3}/\chi^2_{\nu 1} > 1.544$ is seen for all measurements with $Y_3 > 0.48$ (F value for models with 125 data points and 6 and 11 parameters respectively, at a confidence level of 99%). Under these conditions one can decide only by the fit whether more than one component is present in solution. It should be noted that this model can only be applied to determine the mole fractions of the corresponding molecules in solution if detailed information about the diffusion correlation times, the triplet correlation times, and the quantum yields of the fluorophores is available.

Under conditions where this information is lacking, it is in general only possible to decide from the statistics whether one or two components are present in solution if the concentration of the slower molecule is high ($Y > 0.6$). However, the discrimination will get worse when the molecules have a lower fluorescence yield.

Comparison of simulations and experiments

A series of experiments was performed to verify the results of the simulations. As test components, Rho 6G and Rho-

BSA were chosen. The diffusion coefficients match well with the expected values assuming spherical shape of the molecules according to their relative molar masses. (Rho 6G: 479 d; Rho-BSA: 66 kd). The count rate per particle is not identical for both probes. Rho-BSA has a count rate of about 12 kHz per particle and Rho 6G of 30 kHz per particle at the laser power used, corresponding to the high count rate case. Thus these particles can be directly compared to simulations assuming a count rate of 15 kHz per particle. The correlation times differ by a factor of 5, according to the simulations, which is above the limit for distinguishing two components with $Y = 0.5$ and also above the limit for $Y = 0.1$. The experiments showed that different ratios of Rho 6G and Rho-BSA could be fitted with a simple one-particle fit. Only with a fraction of Rho-BSA of about 0.5 was the two-component fit statistically distinguishable from the one-component fit by the F-test. If one takes into account that the count rate per particle is higher for free Rho 6G, this particle fraction comes close to the case where the overall count rate of each particle size is comparable.

To achieve reasonable fitted fractions for the components the correlation time for the two particles, as well as their triplet correlation times, must be held fixed. In this case even below the resolution limit the fraction can be fitted, but doing this requires the additional information that two particles are in solution, which is not available with the experimental data. Another possibility is to use the increase of the correlation time in a one-particle fit, as was done in Klingler et al. (1997). (For comparison, to be able to separate two points with an optical microscope they must be a certain distance apart. The absolute position of one point can be measured more precisely than this resolution. At the limit of resolution, the positions of the two points can be calculated by deconvolution.)

Lateral diffusion: a comparison between FCS and FRAP

FCS and fluorescence recovery after photobleaching (FRAP) have been widely used to determine the lateral diffusion of molecules in biological and artificial membranes. The ranges of applicability of these two methods will be considered here by comparing the concentrations of labeled molecules necessary to obtain good signals, the time domains in which they are useful, and their capabilities to resolve different diffusion constants.

To perform a FRAP experiment at least 100 labeled molecules/μm^2 (Wolf, 1989) are necessary. For an FCS experiment, 1 molecule in the probe volume or less is sufficient, i.e., about 20 times fewer molecules (using a probe diameter of $\omega_1 = 0.25$ μm) than for FRAP. In contrast to FRAP, the signal becomes worse when the concentration is increased in a FCS experiment.

The diffusion coefficient of proteins in natural membranes ($D \approx 10^{-10}$ cm^2/s) can be measured with FRAP and FCS. But FRAP might be better suited for this task because immobile fractions are not detected by FCS and are photobleached over time. Diffusion in lipid bilayers can be measured with both methods. Particles in solution can easily be observed with FCS, but move too fast for FRAP. Thus the big advantage of FCS is the possibility to simultaneously measure particles in solution and bound to membranes. They can be measured with one experiment and can be clearly distinguished.

Gordon et al. (1995) presented a detailed discussion of time resolution in FRAP experiments. They performed simulations of FRAP measurements and calculated the success in discrimination between one- and two-particle diffusion when fitting FRAP data for different signal intensities and different ratios of correlation times. At a medium pre-bleach signal intensity of 316 counts/channel (with a channel width of 20 ms) they showed that the diffusion coefficients should differ by a factor of 10 to identify two-component diffusion unequivocally. In the case of bigger differences they could distinguish the two components, but the error in the diffusion coefficient was large. The relative error (standard deviation divided by the true value) of the slower component was bigger than 1.

In a certain range the time resolution of FCS has definite advantages. FCS is not as well suited as FRAP for the measurement of molecules in natural membranes showing typical diffusion coefficients in the range of 10^{-10} cm^2/s. This corresponds to a correlation time τ_D of about 1 second (see Eq. 3). However, for diffusion of molecules in solution or in lipid bilayers where the diffusion coefficient is between 10^{-6} and 10^{-9} cm^2/s (τ_D between 50 μs and 50 ms) the resolution and accuracy of FCS is much better than that of FRAP.

FCS offers a completely different possibility to determine the aggregation state by counting the absolute number of particles in the probe volume. Knowing the concentration of the monomers, the average aggregation state can be determined (as proposed by Petersen, 1984 for a variant of FCS, the scanning FCS). It has also been proposed to use higher order correlation functions to measure the aggregation based on the value obtained for the autocorrelation function at $\tau = 0$ (Palmer and Thompson, 1989).

CONCLUSIONS

The correlation time resolution of FCS was estimated by the simulation of experiments. It was shown that correlation times should differ by at least a factor of 1.6 to distinguish two particles in the case of a strong fluorescence signal (e.g., rhodamine as a dye). If the signal is weaker (e.g., for [(N-[7-Nitrobenz-2-oxa1,3-diazol-4-yl]) (NBD) where only moderate laser intensities can be used because of a high photobleaching rate) a factor of 8 is necessary to distinguish two molecular species. This makes FCS an interesting method to follow binding of proteins to free and supported lipid layers, for example. It allows discrimination between bound and unbound peptides and simultaneously gives in-

formation about the diffusion coefficients. The measurements show that only under very specific conditions it is feasible to distinguish on a statistical basis whether a solution contains one or two fluorescent species.

If correlation times for diffusion and for triplet states of the components as well as their relative quantum yields, are known, then two-component fits can distinguish between a one- and a two-component solution. However, even this is only possible when the concentration of the second component is high enough compared to the first one. In our measurements this concentration was reached when the fraction of Rho-BSA was higher than 0.5, but this limit will vary with the difference in the diffusion coefficients of the components and their quantum yields. The detection limit of the second molecular species in solution depends critically on the concentration of the molecules and might be lowered using a global fit analysis (Beechem, 1992) if applicable (e.g., for binding measurements). The simulations predict that a factor of at least 1.6 in the diffusion coefficients is necessary to make a distinction between two components. The experiments show that this limit is even greater if the value of Q for the slower component is much smaller than that for the faster component ($\alpha = 0.4$). In addition, these measurements show that the slower component must be present in a certain concentration to be detectable individually.

Nevertheless, if aggregation or binding processes in the sample are expected, the correlation time obtained from a one-component fit can indicate aggregation or binding, as shown by these and other experiments (Klingler et al., 1997). This is possible because the correlation time for a one-component fit is the weighted average of the correlation times of the fluorescent molecules in solution. Therefore, we conclude that FCS can be used to indicate binding or aggregation using a one-component model. But it gives no conclusive evidence for the presence of two components in solution unless a two-particle fit can be used with detailed knowledge of the photophysical properties of both molecules present.

Quantification of FCS data in terms of binding or aggregation requires knowledge of the fluorescence characteristics of the fluorescent molecules in the free and bound/aggregated state. Otherwise, two-particle fits will not yield physically reasonable values. In addition, there exists a concentration threshold under which aggregation and binding can not be proven with statistical certainty.

All simulations of and fits to experimental data have been performed using the model of Koppel (1974) because to our knowledge all published measurements were evaluated by this model. Therefore, our results should be directly applicable to all FCS measurements. Nevertheless, this model is only qualitatively correct. A new way to calculate the variance of the ACF should be found.

Further studies are in progress performing simulations of the intensity signal. That approach would make it possible to calculate the variance of the ACF directly from the signal, resulting in quantitatively accurate simulations. If at the same time the variance of the measured ACF is calculated from the experimental intensity signal, fitting the data, which is a crucial step in FCS, would be more accurate and the resolution of FCS would be improved.

We thank Jerker Widengren and Ülo Mets for introducing Ulrich Meseth to the technique of FCS during a stay at the Karolinska Institute, Stockholm, Sweden.

Supported by the Swiss National Science Foundation, SPP Biotechnology, 5002-235180 (H. V.), and by the Swedish Natural Science Research Foundation and Technical Research Foundation (R. R.).

REFERENCES

Aragon, S. R., and R. Pecora. 1976. Fluorescence correlation spectroscopy as a probe of molecular dynamics. *J. Chem. Phys.* 64:1791–1803.

Basché, T. 1996. Quantenoptische Experimente mit einzelnen Molekülen. *Phys. Bull.* 52:456–459.

Beechem, J. M. 1992. Global analysis of biochemical and biophysical data. *In* Methods in Enzymology: Numerical Computer Methods, Vol. 210. L. Brand and M. L. Johnson, editors. Academic Press, Inc., New York. 37–54.

Berland, K. M., P. T. C. So, and E. Gratton. 1995. Two-photon fluorescence correlation spectroscopy: Method and application to the intracellular environment. *Biophys. J.* 68:694–701.

Bevington, P. R., and D. K. Robinson. 1992. Data Reduction and Error Analysis for the Physical Sciences. McGraw Hill, New York.

Ehrenberg, M., and R. Rigler. 1974. Rotational brownian motion and fluorescence intensity fluctuations. *Chem. Phys.* 4:390–401.

Ehrenberg, M., and R. Rigler. 1976. Fluorescence correlation spectroscopy applied to rotational diffusion of macromolecules. *Q. Rev. Biophys.* 9:69–81.

Elson, E. L., and D. Madge. 1974. Fluorescence correlation spectroscopy: conceptual basis and theory. *Biopolymers.* 13:1–27.

Gordon, G. W., B. Chazotte, X. F. Wang, and B. Herman. 1995. Analysis of simulated and experimental fluorescence recovery after photobleaching: data for two diffusing components. *Biophys. J.* 68: 766–778.

Hinterdorfer, P., H. J. Gruber, J. Striessnig, H. Glossmann, and H. Schindler. 1997. Analysis of membrane protein self-association in lipid systems by fluorescence particle counting: application to the dihydropyridin receptor. *Biochemistry.* 36:4497–4504.

Huang, Z., and N. L. Thompson. 1996. Imaging fluorescence correlation spectroscopy: nonuniform IgE distributions on planar membranes. *Biophys. J.* 70:2001–2007.

Icenogle, R. D., and E. L. Elson. 1983. Fluorescence correlation spectroscopy and photobleaching recovery of multiple binding reactions. I. Theory and FCS measurements. *Biopolymers.* 22:1919–1948.

Kask, P., R. Gunther, and P. Axhausen. 1997. Statistical accuracy in fluorescence fluctuation experiments. *Eur. Biophys. J.* 25:163–169.

Kask, P., P. Piksarv, and Ü. Mets. 1985. Fluorescence correlation spectroscopy in the nanosecond time range: photon antibunching in dye fluorescence. *Eur. Biophys. J.* 12:163–166.

Kask, P., P. Piksarv, M. Pooga, Ü. Mets, and E. Lippmaa. 1989. Separation of the rotational contribution in fluorescence correlation experiments. *Biophys. J.* 55:213–220.

Keller, H. E. 1995. Objective lenses for confocal microscopy. *In* Handbook of Biological Confocal Microscopy, 2nd ed. J. B. Pawley, editor. Plenum Press, New York. 111–126.

Klingler, J., and T. Friedrich. 1997. Site-specific interaction of thrombin and inhibitors observed by fluorescence correlation spectroscopy. *Biophys. J.* 73:2195–2200.

Koppel, D. E. 1974. Statistical accuracy in flurescence correlation spectroscopy. *Phys. Rev. A.* 10:1938–1945.

Madge, D., E. L. Elson, and W. W. Webb. 1974. Fluorescence correlation spectroscopy. II. Experimental realization. *Biopolymers.* 13:1–27.

Meseth, U. 1996. Structural and functional investigations of channel forming peptides in lipid membranes. Ph.D. thesis. Ecole Polytechnique Fédéral de Lausanne. 95–140.

Meyer, T., and H. Schindler. 1988. Particle counting by fluorescence correlation spectroscopy. *Biophys. J.* 54:983–993.

Palmer, A. G., and N. L. Thompson. 1989. Fluorescence correlation spectroscopy for detecting submicroscopic cluster of fluorescent molecules in membranes. *Chem. Phys. Lipids.* 50:253–270.

Petersen, N. O. 1984. Diffusion and aggregation in biological membranes. *Can. J. Biochem. Cell Biol.* 62:1158–1166.

Qian, H. 1990. On the statistics of flourescence correlation spectroscopy. *Biophys. Chem.* 38:49–57.

Rauer, B., E. Neumann, J. Widengren, and R. Rigler. 1996. Fluorescence correlation spectrometry of the interaction kinetics of tetramethylrhodamin α-bungarotoxin with *Torpedo califonica* acetylchoine receptor. *Biophys. Chem.* 58:3–12.

Rigler, R., U. Mets, J. Widengren, and P. Kask. 1993. Fluorescence correlation spectroscopy with high count rate and low-background: analysis of translational diffusion. *Eur. Biophys. J.* 22:169–175.

Rigler, R., J. Widengren, and Ü. Mets. 1992. Interactions and kinetics of single molecules as observed by fluorescence correlation spectroscopy. *In* Fluorescence Spectroscopy. O. S. Wolfbeis, editor. Springer-Verlag, Berlin/Heidelberg/New York. 13–24.

Song, L. L., R. P. M. Vangijlswijk, I. T. Young, and H. J. Tanke. 1997. Influence of fluorochrome labeling density on the photobleaching kinetics of fluorescein in microscopy. *Cytometry.* 27:213–223.

Straume, M., and M. L. Johnson. 1992. Analysis of residuals: criteria for determining goodness-of-fit. *In* Methods in Enzymology: Numerical Computer Methods, Vol. 210. L. Brand and M. L. Johnson, editors. Academic Press, New York. 87–105.

Tanford, C. 1961. Physical Chemistry of Macromolecules. John Wiley & Sons, New York.

Thompson, N. L. 1991. Fluorescence correlation spectroscopy. *In* Topics in Fluorescence Spectroscopy, Volume 1: Techniques. J. R. Lakowicz, editor. Plenum Press, New York. 337–378.

Widengren, J. 1996. Fluorescence correlation spectroscopy, photophysical aspects and applications. Ph.D. thesis. Karolinska Institute, Stockholm, Sweden. 66 pp.

Widengren, J., Ü. Mets, and R. Rigler. 1995. Fluorescence correlation spectroscopy of triplet states in solution: a theoretical and experimental study. *J. Phys. Chem.* 99:13368–13379.

Widengren, J., R. Rigler, and Ü. Mets. 1994. Triplet-state monitoring by fluorescence correlation spectroscopy. *J. Fluorescence.* 4:255–258.

Wolf, D. E. 1989. Design, building and use of a fluorescence recovery after photobleaching instrument. *In* Fluorescence Microscopy of Living Cells in Culture, Part B. Quantitative Fluorescence Microscopy: Imaging and Spectroscopy, Vol. 30. D. L. Taylor and Y.-L. Wang, editors. Academic Press, San Diego. 271–306.